Published in final edited form as:

Nat Mater. 2014 December ; 13(12): 1108–1114. doi:10.1038/nmat4066.

Ultrasoft microgels displaying emergent, platelet-like, behaviors

Ashley C. Brown[#1,2], **Sarah E. Stabenfeldt**[#3], **Byungwook Ahn**[1,4], **Riley T. Hannan**[1], **Kabir S. Dhada**[2], **Emily S. Herman**[2], **Victoria Stefanelli**[1], **Nina Guzzetta**[5], **Alexander Alexeev**[6], **Wilbur A. Lam**[1,4,7], **L. Andrew Lyon**[+,2,7], and **Thomas H. Barker**[+,1,7]

[1]The Wallace H. Coulter Department of Biomedical Engineering, Georgia Institute of Technology and Emory University, Atlanta GA 30332

[2]School of Chemistry and Biochemistry, Georgia Institute of Technology, Atlanta, GA 30332

[3]School of Biological and Health Systems Engineering, Arizona State University, Tempe, Arizona 85287

[4]Department of Pediatrics, Division of Pediatric Hematology/Oncology, Aflac Cancer Center and Blood Disorders Service of Children's Healthcare of Atlanta, Emory University School of Medicine, Atlanta, Georgia, USA

[5]Department of Pediatrics, Division of Pediatric Cardiology, Children's Healthcare of Atlanta, Emory University School of Medicine, Atlanta, Georgia, USA

[6]The George W. Woodruff School of Mechanical Engineering, Georgia Institute of Technology, Atlanta, GA 30332

[7]The Parker H. Petit Institute for Bioengineering and Biosciences, Georgia Institute of Technology, Atlanta, GA 30332

[#] These authors contributed equally to this work.

Efforts to create platelet-like structures for the augmentation of hemostasis have focused solely on recapitulating aspects of platelet adhesion [1]; more complex platelet behaviors such as clot contraction [2] are assumed to be inaccessible to synthetic systems. Here, we report the creation of fully synthetic platelet-like particles (PLPs) that augment clotting in vitro under physiological flow conditions and achieve wound-triggered hemostasis and decreased bleeding times in vivo in a traumatic injury model. PLPs were synthesized by combining highly deformable microgel particles with molecular-recognition motifs identified through directed evolution. In vitro and in silico analyses demonstrate that PLPs actively collapse fibrin networks, an emergent behavior that mimics in vivo clot contraction. Mechanistically, clot collapse is intimately linked to the PLP's unique deformability and affinity for fibrin

[+]Corresponding Authors: Thomas H. Barker, Ph.D. Address: The Wallace H. Coulter Department of Biomedical Engineering at Georgia Tech and Emory University, 313 Ferst Drive, Suite 2108, Atlanta, GA 30332-0535 (404) 385-5039 – phone (404) 894-4243 – fax thomas.barker@bme.gatech.edu L. Andrew Lyon, Ph.D. Address: Georgia Institute of Technology, School of Chemistry and Biochemistry, 901 Atlantic Dr. NW, Atlanta, GA 30332-0400 (404) 894-4090 – phone (404) 894-7452 – fax lyon@gatech.edu.

Contributions ACB, SES, BA experimental design, data analysis and manuscript; RTH, KSD, ESH, VS experimental design and data analysis; AA, simulations, data analysis and manuscript; NG, WAL, LAL, and THB, experimental design and manuscript.

fibers, as evidenced by dissipative particle dynamics simulations. Our findings should inform the future design of a broader class of dynamic, biosynthetic composite materials.

Uncontrolled bleeding is the major cause of death in civilian and battlefield traumas [3,4], highlighting the critical need for better technologies for wound management. Current hemostasis technologies including topical sealants, exothermic zeolites, advanced dressings and recombinant clotting factors [5,6] have demonstrated modest successes, yet all have significant drawbacks and none are as “evolved” as the natural hemostasis system. More recent efforts have focused on creation of synthetic analogs of clotting constituents, most notably platelets. The vital platelet functions [2,7] that one would like to recapitulate include 1) binding, stabilization, and enhancement of fibrin clot formation in dynamic flow conditions, 2) clot contraction and 3) cytokine and growth factor release to stimulate wound healing. To date, all artificial platelet approaches ranging from purely synthetic to reconstituted freeze-dried harvested native platelets fail to fully recapitulate these key functions. Most approaches claiming success achieve only the binding and augmentation of clot formation through multivalent display of platelet-binding motifs or platelet-cell surface adhesion motifs on a micro/nano-sized vehicle [1].

Such approaches are sufficient to recruit clotting components and thereby decrease clotting time, however, these studies rely upon vehicles that lack the natural platelet's ability to deform within and in response to the fibrin mesh. To more accurately mimic platelet function, we created a highly deformable platelet “body” that enables multivalent display with much greater conformational flexibility. To that end, ultra-low cross-linked (ULC) poly(*N*-isopropylacrylamide-*co*-acrylic acid) (pNIPAm-AAc) microgels (μgels) were synthesized via a nonstandard, `cross-linker free', precipitation polymerization method [8]. This unique method leverages rare chain transfer associated chain branching events to create μgels with exceedingly low (<0.5%), core-localized, cross-linking densities resulting in particles with an unmatched deformability [9]. Like natural platelets, ULC μgels are ~1 μm in diameter in solution. Upon initiation of clotting, platelets become activated, bind to nascent fibrin fibers, actively spread within the fibrin network, and over time engage their actin-myosin machinery to contract the clot (Figure 1A). Through the course of these events, platelets undergo significant shape changes. Our ULC μgel platelet “bodies” are capable of undergoing large degrees of deformation as suggested by AFM images of μgels spread on a glass surface with a diameter of approximately 2 μm but an approximate height of only 4 nm.

The μgels were enabled with clot specificity via evolved variable domain-like recognition motifs (sdFv) displaying high selectivity for nascent fibrin protofibrils and minimal binding to the soluble circulating precursor, fibrinogen. Fibrin specificity is a critical design feature of our platelet-like particles (PLPs), as it allows for unrivaled specific targeting to a wound site without nonspecific interactions with the soluble precursor fibrinogen or circulating platelets. This seemingly simplistic approach is critically complicated by the molecular homology between fibrin and fibrinogen molecules; previous fibrin targeting attempts are also known to interact to some degree with fibrinogen domains [10–12]. We overcame this challenge and successfully identified fibrin-specific sdFvs through phage display biopanning. We performed screens with three different phagemid libraries [13] *in vitro* against

fibrin clots. Following three rounds of screening (figure S1), 96 clones from each library were tested for binding to fibrin and fibrinogen (figure S2). The four most promising clones, based on their selectivity for fibrin over fibrinogen, and a random clone were then evaluated through SPR (figure S3). The clone found to have the highest affinity for fibrin (H6), and the random, nonbinding clone (S11) were utilized for creation of PLPs and control particles, respectively. Interferometery analysis verified that H6-μgels, the so-called PLPs, maintained their fibrin-binding capabilities (figure 1C), while no binding of S11-μgels (control PLPs) to fibrin was observed.

To first investigate the ability of our PLPs to recapitulate platelet function, we tested clotting of platelet-poor plasma in relation to platelet-rich plasma *in vitro*. These dynamic clotting experiments were performed in an endothelialized microfluidic device that recapitulates the cellular, physical, and hemodynamic environment of microcirculation (described in detail in supplemental methods) [14]. As is widely accepted, we found that normal human platelet-rich plasma under flow conditions displays robust formation of a fibrin-based clot in the presence of thrombin whereas the depletion of platelets diminishes this response. Supplementation of platelet-poor plasma with PLPs successfully rescued fibrin clot formation in response to thrombin, even in 1:1 saline-diluted platelet-poor plasma (figure 2 and videos 1–5). This triggered response was presumed to be an effect of multivalent presentation of the fibrin-specific sdFv only. Indeed, particle deformability does not appear critical to this effect since H6-particles with higher degrees of cross-linking (decreased deformability) support thrombin-induced clot formation in platelet-poor plasma (figure S4). PLPs are additionally able to augment clotting in post-surgical platelet-poor plasma from neonates undergoing cardio-pulmonary bypass to correct congenital defects (figure S5). This challenging population has an underdeveloped coagulation system and experiences additional coagulopathy induced by plasma dilution effects of the cardiopulmonary bypass machine [15]. In contrast, PLPs cannot augment clotting in severe hemophilia patients in which a FVIII/FIX deficiency prevents formation of fibrin, the PLP `trigger'.

In addition to augmenting fibrin formation, PLPs spread significantly within fibrin matrices, similarly to levels seen with natural platelets (figure 3A), while non-binding S11-ULC or hard H6-polystyrene (PS) particles spread significantly less than PLPs. Surprisingly, clots formed in the presence of PLPs were found to have a significantly altered structure. These clots were highly heterogeneous, containing regions of dense fibrin observed in conjunction with PLPs (figure 3B), with the dense features becoming more pronounced over time, similar to features observed from clots formed from platelet-rich plasma, although occurring on a different time scale. Clots formed in the presence of non-binding S11-ULC μgels were found to result in a more porous network compared to control (i.e. fibrin-only) clots, but the structure remained largely homogenous, and was similar to fibrin-only clots. We next characterized clot collapse at the macroscopic level by performing standard gross clot contraction experiments routinely utilized by platelet biologists [16,17]. Clot collapse was observed within 24 – 48 hours in the presence of PLPs but not under any other conditions tested (figure 3C). No significant differences in the overall degree of clot collapse were observed when comparing platelet-poor plasma containing PLPs and native platelet-rich plasma (figure 3D). However, not surprisingly, the rate of PLP-induced collapse was slower

than that observed in native platelet-containing clots. We analyzed the role of particle deformability in the observed alterations in clot structure by comparing clots formed in the presence of PLPs, 2% BIS, 4% BIS, or 7% BIS μgels, or PS particles conjugated to the fibrin-specific sdFv and found that only PLPs significantly altered clot structure at both the microscopic (Figure S6) and macroscopic level (Figure S7). These results suggest that fibrin binding coupled with high levels of particle deformability likely contribute to the significant alterations in clot structure observed. Clot contraction is a significant function of natural platelets and has been correlated to enhanced clot stability, decreased fibrinolysis and is a strong contributing factor to subsequent wound healing [18]. Similarly, clots formed in the presence of PLPs were more resistant to degradation than control clots or clots formed in the presence of S11-ULC μgels (figure S7). It should be noted that the role of gross clot collapse mediated by natural platelets is not a primary contributor to initial clot formation but rather occurs after establishment of the platelet-fibrin hemostatic plug.

To gain insight into the mechanisms by which PLPs contribute to macroscopic clot collapse, we developed a computational model of a compliant polymer network interacting with soft, deformable particles (figure 3E and video 6). Non-adhesive particles have no effect on network size. However, even weak attraction between particles and network filaments led to a significant reduction of the network size. When particles attach to the network, they join neighboring filaments (figure 3G), leading to local alterations in microstructure that not only disrupt network homogeneity, but also reduce its stability, which in turn ultimately causes compete network collapse (figure 3F). Local collapse is governed by the interplay between network elasticity and particle adhesiveness; more adhesive particles cause faster network collapse (figure 3H). Furthermore, our simulations confirm that particle compliance plays a key role in network collapse. Networks seeded with softer particles show a larger degree of collapse than those with stiff particles (figure S7 and video 7). This can be related to a higher ability of soft particles to form intimate contacts with network fibers (figure 3G), thereby reducing the energy barrier for clot collapse.

Lastly, we tested PLPs' ability to recapitulate the important platelet function of augmenting clotting *in vivo* and homing to sites of injury by utilizing a well-established rat femoral vessel traumatic injury model [19–21]. Experimental groups or vehicle were injected intravenously and allowed to circulate for five minutes prior to induction of injury to the femoral vein. Bleeding time following injury was found to significantly decrease in the presence of PLPs ($p<0.01$) compared to vehicle only and were similar to those in the presence of the current clinical standard, Factor VIIa. PLPs resulted in a more significant reduction in bleeding time than transfusion of 100-fold greater numbers of infused fresh platelets (figure S8). S11-ULC μgels did not significantly affect bleeding times compared to vehicle only control (figure 4), and total blood loss was significantly less in the presence PLPs compared to S11-ULC μgels ($p<0.05$). Analysis of bleeding dynamics also demonstrated that PLPs resulted in the slowest blood loss over time, while S11-ULC μgels resulted in the most rapid blood loss (figure 4C–D). Wound tissue was analyzed postmortem for fibrin and PLP deposition through MSB staining for fibrin and immunohistochemical staining for the MYC-tag encoded on the sdFvs. Co-localization of PLPs within fibrin clots (figure 4D, arrows) was observed, while minimal MYC staining was observed in S11-ULC

μgels tissue samples. Furthermore, higher levels of fibrin staining were observed in vessels collected from animals receiving PLPs. These data indicate that PLPs are capable of localizing to the site of injury, enhancing fibrin clot formation, and decreasing bleeding time and blood loss.

We demonstrate that our PLPs can recapitulate some key functions of platelets including binding, stabilizing and enhancing fibrin clot formation, responsiveness to injury cues, and induction of clot collapse. To our knowledge, no platelet-mimetic materials recapitulate all of these important functions of platelets involved in hemostasis. It should be noted that several differences exist between our PLPs and natural platelets. While PLPs bind only fibrin, resting platelets bind neither fibrinogen nor fibrin, but activated platelets bind both and serve as initiators of wound healing. Furthermore, natural platelets serve as a platform for recruitment of procoagulant factors that enhance the hemostatic response and actively generate thrombin on their surfaces, resulting in fibrin fibers originating from platelet aggregates. Platelet phosphatidyl serine also contributes to this response by binding plasma coagulation proteins. PLPs bind nascent fibrin fibers, serving predominantly as nucleating agents and cross-linkers during clot formation, and are trapped within the network. In other words, platelets initiate clotting, while PLPs enhance fibrin formation that has already begun. This is a nice advantage of our system since PLPs should not initiate adverse clot formation; our data with hemophilia patients further supports this premise.

Perhaps the most exciting, and surprising, result generated by our approach is the ability to induce clot collapse without the active contractile machinery required for natural platelet-mediated clot contraction. In the native platelet, ATP-driven actinomyosin mediated contraction enables rapid collapse over a few hours while ATP-independent collapse resulting from our PLPs occurs on a much longer time scale (tens of hours). The multivalent interactions between μgel polymer chains and fibrin fibers likely cause local deformation of the fibrin network, acting as cross-linkers or bridging sites between adjacent fibers. Such bridging sites likely make subsequent μgel binding more favorable via a cooperative “zipper effect” [22–24]. Over time these multiple small collapses and concomitant μgel binding will lead to an overall (macroscopically observable) network collapse. Recent studies characterizing collapse of actin polymers by myosin demonstrate that actin network connectivity (determined by the degree of cross-linking) controls length scales of collapse, with weakly connected networks contracting locally, medially cross-linked networks contracting into multiple disjointed clusters, and strongly cross-linked networks contracting into a single dense cluster [25]. We observe a similar phenomenon in our fibrin-PLP systems, however in our system, the collapse changes over time as the PLPs, presumably, increase the degree of network connectivity. Over time, we observe that PLPs induce local network collapse, followed by collapse into multiple dense fibrin clusters, ultimately inducing collapse into a single dense fibrin cluster. A few features of the PLPs appear to be critical for this process. First, the high fibrin affinity imparted by H6 permits the particles to remain bound to the fibers as the clot collapses. Second, the extremely low density of the ULC μgels likely permits the pendant sdFvs to engage fibrin with near-native affinity. In contrast, more densely cross-linked (and therefore not as deformable) particles would restrict the ability of pendant sdFvs to bind to multiple fibers, therefore decreasing the degree of fiber deformation and diminishing the cooperativity of subsequent μgel binding events. This is

supported by our clot collapse simulations, which demonstrate that loosely cross-linked particles take on multiple conformations to interact with the fibrin network and induce clot collapse to a greater degree than non-deformable hard particles. It is also possible that PLP binding to preformed fibrin oligomers and subsequent assembly of the network introduces an uneven distribution of tension in the network, resulting in instabilities that further contribute to network collapse.

Our ability to recapitulate many functions of natural platelets demonstrates the power of evolution-based approaches in designing biomimetic biomaterials. Although this report specifically focuses on PLPs and their emergent dynamic behaviors, we believe that the use of ultra-soft/deformable colloidal systems represents a unique strategy toward the development of a new class of biosynthetic composite materials whose component parts more intimately engage and augment one another.

Methods

Evolution of high affinity fibrin-specific sdFvs and creation of PLPs

Variable domain-like recognition motifs (sdFv) or single chain antibodies with high affinity for fibrin were identified using three phagemid libraries in biopanning assays against fibrin. Fibrin specificity was evaluated via fibrinogen and fibrin-based enzyme-linked immunosorbent assays. Clones with high affinity for fibrin and low affinity for fibrinogen were produced, purified and fibrin binding kinetics were evaluated through surface plasmon resonance. The clone with the highest affinity for fibrin, clone H6, was then coupled to ULC μgels for creation of PLPs. Negative control particles were created by coupling a random, non-fibrin binding sdFv clone to ULC μgels.

In vitro and *in silico* analysis of PLPs

To characterize the effect of PLPs on clotting *in vitro*, we utilized an endothelialized microfluidic device that recapitulates the cellular, physical, and hemodynamic environment of microcirculation, similar to a device previously described[26,27]. For these experiments, clotting of platelet poor plasma was analyzed in the absence or presence of PLPs in real time using confocal microscopy. Microscopic analysis of fibrin clot structure in the presence or absence of PLPs was also performed using confocal microscopy. Macroscopic clot deformation was analyzed through gross clot collapse assays. H6-μgels with varying degrees of crosslinking or S11-ULC μgels were added to the clots prior to addition of thrombin. *In silico* analysis was then performed with dissipative particle dynamics (DPD)[28–30] to examine the dynamic response of fibrin network interacting with soft and stiff particles.

In vivo analysis of hemostatic functions of PLPs—To test the efficacy of PLPs in hemostasis, we utilized a rat femoral vessel traumatic injury model[19–21]. Co-localization of PLPs were characterized postmortem through immunofluorescence staining for the MYC-tag encoded on the sdFvs and through Martius Scarlet Blue (MSB) staining for fibrin in adjacent serial sections.

Methods are described in detail in supplementary information.

Supplementary Material

Refer to Web version on PubMed Central for supplementary material.

Acknowledgements

The authors wish to thank Ms. Laura Tucker and Mrs. Sarah Pitrowski Lees for assistance with *in vivo* studies, Mr. Allen Winburn for assistance with particle synthesis, Dr. Zhiyong Meng for AFM images of ULC μgels films, and Ms. Yumiko Sakuri, Dr. Yong Qui and Dr. David Myers for assistance with platelet poor plasma isolation. Funding sources: NIH (HHSN268201000043C, R21EB013743 and R01EB011566), John and Mary Brock Discovery Research Fund, and DoD (W81XWH1110306) to THB; NIH (R21EB013743) and DoD (W81XWH1110306) to LAL; American Heart Association Postdoctoral Fellowship to ACB; NSF GRF to VS; NSF CAREER Award (DMR-1255288) to AA; NIH (R01HL121264, U54 HL11230 and NSF CAREER Award (1150235) to WL.

References

1. Modery-Pawlowski CL, et al. Approaches to synthetic platelet analogs. Biomaterials. 2013; 34:526–541. doi:Doi 10.1016/J.Biomaterials.2012.09.074. [PubMed: 23092864]
2. Clemetson KJ. Platelets and primary haemostasis. Thrombosis research. 2012; 129:220–224. doi: 10.1016/j.thromres.2011.11.036. [PubMed: 22178577]
3. Evans JA, et al. Epidemiology of traumatic deaths: comprehensive population-based assessment. World journal of surgery. 2010; 34:158–163. doi:10.1007/s00268-009-0266-1. [PubMed: 19882185]
4. McGwin G Jr. et al. Reassessment of the tri-modal mortality distribution in the presence of a regional trauma system. J Trauma. 2009; 66:526–530. doi:10.1097/TA.0b013e3181623321. [PubMed: 19204533]
5. Geeraedts LM Jr. Kaasjager HA, van Vugt AB, Frolke JP. Exsanguination in trauma: A review of diagnostics and treatment options. Injury. 2009; 40:11–20. doi:10.1016/j.injury.2008.10.007. [PubMed: 19135193]
6. Granville-Chapman J, Jacobs N, Midwinter MJ. Pre-hospital haemostatic dressings: a systematic review. Injury. 2011; 42:447–459. doi:10.1016/j.injury.2010.09.037. [PubMed: 21035118]
7. Fries D, Martini WZ. Role of fibrinogen in trauma-induced coagulopathy. British journal of anaesthesia. 2010; 105:116–121. doi:10.1093/bja/aeq161. [PubMed: 20627882]
8. Gao JF, B.J. Cross-linker-free N-isopropylacrylamide gel nanospheres. Langmuir : the ACS journal of surfaces and colloids. 2003; 19:5212–5216.
9. Hendrickson GR, Lyon LA. Microgel Translocation through Pores under Confinement. Angew Chem Int Edit. 2010; 49:2193–2197. doi:Doi 10.1002/Anie.200906606.
10. Raut S, Gaffney PJ. Evaluation of the fibrin binding profile of two anti-fibrin monoclonal antibodies. Thrombosis and haemostasis. 1996; 76:56–64. [PubMed: 8819252]
11. Kolodziej AF, et al. Fibrin specific peptides derived by phage display: characterization of peptides and conjugates for imaging. Bioconjugate chemistry. 2012; 23:548–556. doi:10.1021/bc200613e. [PubMed: 22263840]
12. Scheefers-Borchel U, Muller-Berghaus G, Fuhge P, Eberle R, Heimburger N. Discrimination between fibrin and fibrinogen by a monoclonal antibody against a synthetic peptide. Proceedings of the National Academy of Sciences of the United States of America. 1985; 82:7091–7095. [PubMed: 2413458]
13. Lee CM, Iorno N, Sierro F, Christ D. Selection of human antibody fragments by phage display. Nature protocols. 2007; 2:3001–3008. doi:10.1038/nprot.2007.448. [PubMed: 18007636]
14. Myers DR, et al. Endothelialized microfluidics for studying microvascular interactions in hematologic diseases. Journal of visualized experiments : JoVE. 2012 doi:10.3791/3958.
15. Guzzetta NA, et al. The impact of aprotinin on postoperative renal dysfunction in neonates undergoing cardiopulmonary bypass: a retrospective analysis. Anesthesia and analgesia. 2009; 108:448–455. doi:10.1213/ane.0b013e318194007a. [PubMed: 19151271]

16. Thomas SG, Calaminus SD, Auger JM, Watson SP, Machesky LM. Studies on the actin-binding protein HS1 in platelets. BMC cell biology. 2007; 8:46. doi:10.1186/1471-2121-8-46. [PubMed: 17996076]
17. Suzuki-Inoue K, et al. Involvement of Src kinases and PLCgamma2 in clot retraction. Thrombosis research. 2007; 120:251–258. doi:10.1016/j.thromres.2006.09.003. [PubMed: 17055557]
18. Jackson SP, Nesbitt WS, Westein E. Dynamics of platelet thrombus formation. Journal of thrombosis and haemostasis : JTH. 2009; 7(Suppl 1):17–20. doi:10.1111/j.1538-7836.2009.03401.x. [PubMed: 19630759]
19. Bertram JP, et al. Intravenous hemostat: nanotechnology to halt bleeding. Science translational medicine. 2009; 1:11ra22. doi:10.1126/scitranslmed.3000397.
20. Fuglsang J, et al. Platelet activity and in vivo arterial thrombus formation in rats with mild hyperhomocysteinaemia. Blood coagulation & fibrinolysis : an international journal in haemostasis and thrombosis. 2002; 13:683–689. [PubMed: 12441906]
21. Ersoy G, et al. Hemostatic effects of microporous polysaccharide hemosphere in a rat model with severe femoral artery bleeding. Advances in therapy. 2007; 24:485–492. [PubMed: 17660156]
22. Okano, T.; Y. H. B.; Kim, SW. In Modulated Control Release System. Kost, J., editor. CRC Press; 1990. p. 17
23. Tsuchida, E.; Abe, K. Advances in Polymer Science. Vol. Vol. 45. Springer; Berlin: 1982. p. 1-119.
24. Shibayama, M.; Tanaka, T. Responsive Gels: Volume Transitions 1. Dusek, K., editor. Vol. Vol. 109. Springer; 1993. p. 1-62.
25. Alvarado J, Sheinman M, Sharma A, MacKintosh F, Koenderink G. Molecular motors robustly drive active gels to a critically connected state. Nature Physics. 2013; 9:591–597. doi:10.1038/nphys2715.
26. Tsai M, et al. In vitro modeling of the microvascular occlusion and thrombosis that occur in hematologic diseases using microfluidic technology. The Journal of clinical investigation. 2012; 122:408–418. doi:10.1172/JCI58753. [PubMed: 22156199]
27. Tsai M, et al. In vitro modeling of the microvascular occlusion and thrombosis that occur in hematologic diseases using microfluidic technology. Journal of Clinical Investigation. 2012; 122:408–418. doi:Doi 10.1172/Jci58753. [PubMed: 22156199]
28. Groot RD, Warren PB. Dissipative particle dynamics: Bridging the gap between atomistic and mesoscopic simulation. Journal of Chemical Physics. 1997; 107:4423–4435.
29. Hoogerbrugge PJ, Koelman JMVA. Simulating Microscopic Hydrodynamic Phenomena with Dissipative Particle Dynamics. Europhys Lett. 1992; 19:155–160.
30. Espanol P, Warren P. Statistical-Mechanics of Dissipative Particle Dynamics. Europhys Lett. 1995; 30:191–196.

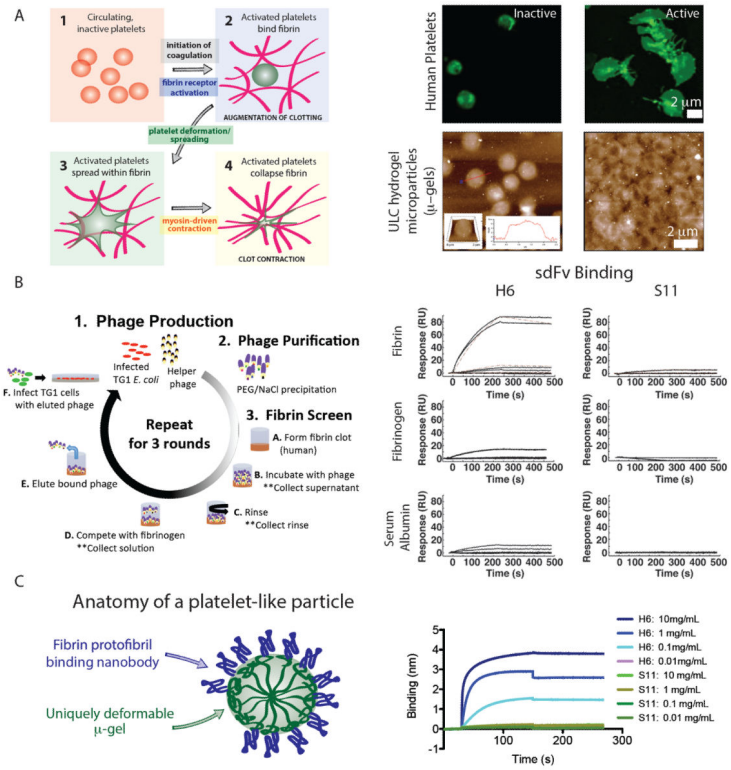

Fig 1. PLP design and characterization

(A) Mimicking platelet features: Upon activation, circulating platelets spread extensively within fibrin matrices and undergo significant shape changes. A schematic of this activation and spreading is shown. Human platelets were isolated, stained with a cell membrane dye (Cell Mask Green), plated on fibrinogen-coated surfaces for two hours, then fixed and imaged via confocal microscopy. To induce activation, platelets were incubated with α-thrombin. Like human platelets, ULC μgels spread extensively and can undergo extensive shape changes as seen via AFM images of ULC μgels plated at various densities. (B) Schematic outlining phage biopanning against fibrin. Fibrin binding kinetics of promising sdFvs were evaluated via SPR. Representative SPR sensorgrams of fibrin-binding (H6) or random clone (S11) sdFvs binding to a thin fibrin layer, fibrinogen surface or BSA surface. (C) H6 sdFvs were conjugated to ULC μgels to produce platelet-like particles (PLPs). The fibrin-specific binding of ULC μgels conjugated to fibrin binding (H6) or non-binding (S11) sdFvs was analyzed through interferometry on fibrin-coated surfaces.

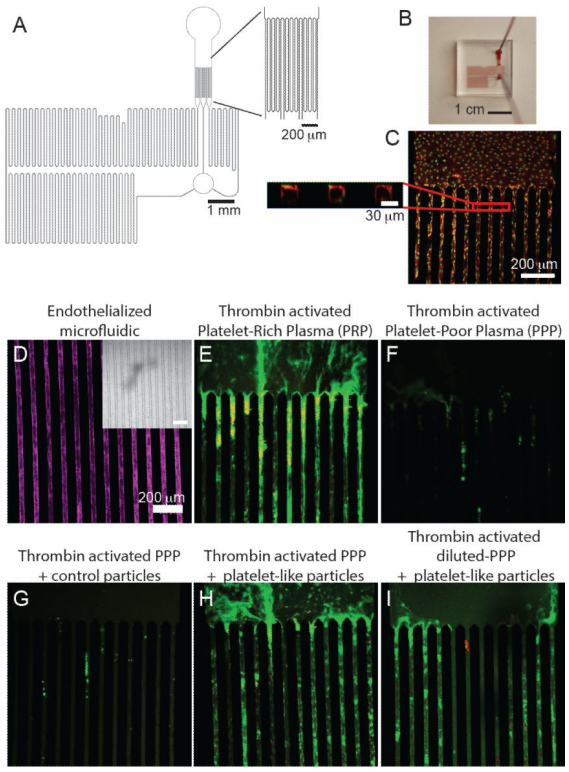

Fig 2. PLPs include clotting in vitro

Endothelialized microfluidic device characterization: a schematic of the device (A) and macroscopic image (B). Endothelial cells were stained with cell mask deep red and nuclei were stained with Syto 13 then imaged via confocal microscopy. Maximum intensity projections and cross-sectional views of the cellularized channels are shown (C). Devices were then utilized to analyze dynamic clotting of platelet rich plasma (PRP) or platelet poor plasma (PPP). Endothelial cells prior to plasma injection stained with cell mask deep red (D) and phase (inset). Clotting of PRP (E), PPP alone (F), PPP + non-fibrin binding microgels (G), PPP + PLPs (H) and diluted PPP + PLPs (I). Fibrin=green; microscaffolds/platelets=red

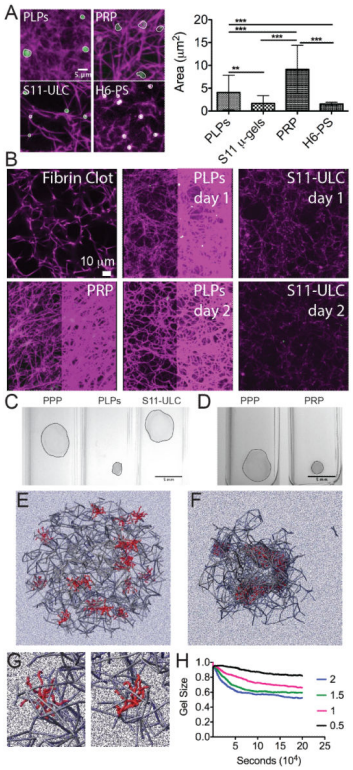

Fig 3. PLPs induce clot collapse in vitro

Maximum intensity confocal images of fibrin clots formed from platelet rich plasma (PRP) or platelet poor plasma (PPP) in the absence or presence of PLPs or S11-ULCs analyzed 1 or 24 hours post-polymerization. Due to increased fibrin density in PRP and PLP clots, equivalent exposure times as fibrin only and S11-ULC clots, resulted in signal saturation. To allow for appreciation of network structure, equivalent exposures are shown on the right and 0.33x exposure are shown on the left for PRP and PLP clots; Fibrin=magenta, Microgels/platelets=green (A). Increased magnification images of PLP, natural platelets (PRP), S11-ULCs and H6-PS spreading within fibrin matrices 1 or 24 hours hour post-polymerization and calculated spread area (B; *** $p<0.001$). Macroscopic collapse of clots formed from PPP in the presence or absence of PLPs or S11-ULCs 48 hours post polymerization (C). Collapse of clots formed from PRP and PPP 4 hours post polymerization (D). Clot collapse simulation results with flexible, loosely cross-linked, binding particles embedded in fibrin network at the beginning (E) and end (F) of the simulation. Images of particles at various locations in the network (G) and the effect of particle affinity for the fibrin network on clot size over time (H).

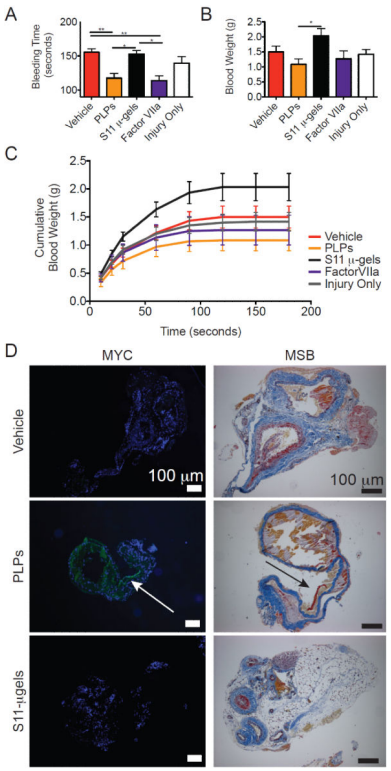

Fig 4. PLPs decrease bleeding time in vivo and home to site of injury

Rats were administered saline (vehicle), PLPs, S11 μgels or Factor VIIa and following a 5-minute circulation time, a femoral vein injury was induced. Bleeding times following injury (A), total blood loss (B), blood loss at various time points (C) and cumulative blood loss over time (D) are presented. Femoral veins were excised, fixed, paraffin embedded and serial sections were stained for the myc-tag encoded on the sdFvs or for fibrin through MSB staining (E). Myc staining/μgels=green and Hoescht/nuclei=blue. For MSB staining, fibrin=red, collagen=blue and erythrocytes=yellow. Arrows indicate localization of PLPs with deposition of fibrin. ** $p<0.01$, * $p<0.05$